Density-Dependent Equations of State for Metal, Nonmetal, and Transition States for Compressed Mercury Fluid

M. H. Ghatee* and M. Bahadori

Department of Chemistry, Shiraz University, Shiraz, 71454, Iran

Received: July 5, 2003; In Final Form: November 4, 2003

Analytical equations of state are presented for fluid mercury in metal, nonmetal, and in metal−nonmetal transition states. Equations of state for metal and nonmetal states are simple in form but the complexities of the transition state leads to a complex fourth-order equation. The interatomic potential function used to describe the metal state has a hard repulsion wall, and that of the nonmetal state is the same as the potential function of the nonpolar fluid with induced dipole intermolecular interaction. Metal−nonmetal transition occurs in the liquid density range 11−8 g/cm^3, and a density-dependent interaction potential function, which gradually changes from a pure metal interaction to a nonmetal interaction in the transition region, is used. Well-depth and the position of potential minimum are presented as temperature dependent quantities; their calculated values for the metal state are typically within 5.0% and 0.33% of the experimental value, respectively. The calculated well-depth for the nonmetal state is smaller than the experimental value indicating the effect of high pressure $P\rho T$ data used, which pushes a pair of mercury atom further together into the repulsion side. In the transition region, calculated well-depths are 2−3 orders of magnitude larger than those for the metal state and contain a sharp rising edge and a steep falling, having a singularity characteristic of phase transition.

1. Introduction

Mercury has the lowest critical temperature of any fluid metals. Therefore, it has been investigated experimentally with accurate measurements in the critical region. These measurements involve its magnetic, electrical, structural, optical, and thermophysical properties with optimal control of temperature in the critical region.[1] The fundamental difficulty in dealing with fluid metals is that the electronic structures of liquid and gas phases are completely different. The electronic structure of mercury (and other molten metals) at low temperatures can be well approximated by the structure of the solid metals, and thus the thermodynamic properties of metals can be obtained by the same cohesion mechanism of the solid metals. Experimental data clearly represent that mercury near its triple point (at densities larger than 11 g/cm^3) follows the nearly free electron theory of metals that considers the nuclei completely shielded by delocalized electrons.[2] At lower densities (9−8 g/cm^3), the cohesion mechanism of its atoms will be suppressed by a partial localization of electrons and the metallic character is changed to a nonmetal kind and a gradual metal−nonmetal transition (M−NMT) occurs. Recently Nagel et al.[3] have calculated the structure factors of expanded liquid mercury for a wide range of density using the effective pair potential obtained from pseudopotential perturbation theory for liquid metal and by the Lennard-Jones potential for corresponding vapor. Although these pair potentials are valid in the two corresponding limiting cases, their validities are lost for those states that are near M−NMT.[3,4]

In addition, experimental investigations of monovalent liquid cesium and rubidium indicate a gradual metal−nonmetal transition near the critical region, but the properties of this transition for a divalent metal are completely different. In this state, fractions of alkali-metal atoms form chemically bonded dimers; however, mercury because of its 6s^2 closed shell ground electronic state does not undergo such a process. From experimental data, it was concluded that the metal−nonmetal transition in liquid mercury is mainly due to lack of overlapping between the 6s and 6p bands.[5,6,7]

For mercury, data of precise measurements of electrical conductivity,[8] Hall coefficient,[9] NMR studies,[10] sound velocity,[11,12] and equation of state,[13] are available. These data clearly demonstrate that a radical change in the atomic states occurs from phase to phase. For instance, far below the critical point, the liquid is highly conducting but the existing vapor does not. More close to the liquid−vapor critical point, where the distinction between the two existing phases vanishes, the electrical conductivity, Knight shift, and optical properties show that the nonmetal behavior is present in both phases.

The major reason for the prediction of thermodynamic properties of mercury and other metals lie in the fact that the intermolecular interaction highly depends on temperature and density. Density dependence of mercury potential function has been subjected to the critical investigations,[12] by using the experimental structure factor and theoretical modeling.

Near the critical point, especially in the M−NMT region, there is no reliable theoretical method to derive an effective potential function for liquid metals accurately. Indeed, at high densities near the triple point the effective pair potential function, obtained from the nearly free electron model, can reproduce the thermodynamic properties quite well, though it gives less satisfactory results in the expanded liquid metals at low densities. Therefore, the accuracy of theoretical studies on the thermodynamic properties of liquid metals is subjected to the accuracy of pair potential function describing the intermolecular interaction of these metals.

In this study, we present density-dependent equations of state for metal, nonmetal, and metal−nonmetal transition states of

* Corresponding author. Fax: +98 711 228 6008. E-mail: ghatee@sun01.susc.ac.ir.

10.1021/jp035940v CCC: $27.50
Published on Web 03/10/2004

fluid mercury. For the transition state, density-dependent potential functions are applied and successfully determine an equation of state which shows inflection from metal to nonmetal. The density range of the transition state is characterized and the method for accurate determination of molecular parameters of the potential function is investigated.

2. Density Dependent Potential Model

The structure factors of liquid mercury were measured by Tamura and Hosokawa,[14] using X-ray along the liquid−vapor coexisting line. Using these structure factors and performing inversion method, potential functions were extracted by Munejiri et al. in three states: the metal state (1273 K, 10.98 g/cm^3), the metal−nonmetal transition state (1673 K, 9.25 g/cm^3), and the nonmetal state (1803 K, 6.8 g/cm^3).[12] The characteristics feature of the effective pair potential function $\phi(r)$ thus obtained are as follows: (a) the attraction well of ϕ (r) for the metal state is broader than those of the nonmetal state; (b) $\phi(r)$ of the nonmetallic state is similar to the Lennard-Jones (12−6) potential function; (c) the repulsion part of $\phi(r)$ is harder than those of rubidium and cesium; (d) when the state of liquid mercury changes from the metal to the metal−nonmetal transition state, the repulsion part shifts to shorter distance and shifts back as the nonmetal state is approached.

The above three states have been studied also by Okurmura and Yanezawa,[15] who have made progress in describing the bulk viscosity of density-dependent potential systems. Bulk viscosity is a measure of dilatational distortion of a liquid and is important in the case of a compressible liquid.[16,17,18] Since the metal−nonmetal transition does not occur at a definite density, the density-dependent potential function $u(r)$ at all densities becomes the potential function of intermediate density asymptotically. On the other hand, the transition state comprises species interacting either on a metal path or on a nonmetal one. Therefore, over the whole range of density of fluid mercury

$$u(r) = f(\rho)u_1(r) + (1 - f(\rho))u_2(r) \tag{1}$$

where $f(\rho)$ is applied to specify extent of transition from state with potential function $u_1(r)$ to the state with potential function $u_2(r)$.[15] For liquid mercury, metal−nonmetal transition occurs at $\rho \approx 9-8$ g/cm^3. Therefore, $f(\rho)$ has the form

$$f(\rho) = \begin{cases} 1 & \rho \geq 11 \text{ g/cm}^3 \\ (\rho - 8)/3 & (8 < \rho < 11) \text{ g/cm}^3 \\ 0 & \rho < 8 \text{ g/cm}^3 \end{cases} \tag{2}$$

3. Density-Dependent Equation of State

To derive the equation of state for mercury, we follow closely the pervious model for dense liquid cesium metal. The method is outlined as follows while the details can be found elsewhere.[19−21] First, the total interaction potential energy of an N atom-liquid system $U(r_1,r_2, ..., r_N)$ is approximated as the sum of pairwise interaction potential energy $u(r_{ij})$ of the atom i with atom j located at distance r_{ij} in the *liquid state*. The summation is restricted to the nearest neighboring atoms and thus $U(r_1,r_2, ..., r_N) = (N/2)u(r)$, where r is the interatomic distance. [Here, for the time being, we do not include the coordination number. See section 4.] Then, the thermodynamic equation of state is solved for pressure of the system, where the internal energy involves total interaction potential energy and kinetic energy. Finally isotherms are obtained for the three states by application of pair potential specified by eqs 1 and 2.

We apply Lennard-Jones (12−6) potential function to low density with nonmetal character (e.g., the state with u_2). The polarizability of nonmetal mercury shall be appreciably large to follow an inverse power law $1/r^6$. For the metal state specified by pair potential u_1, we apply the LJ (15−9) potential function, which indicates the lesser attraction and hard repulsion interactions characteristics of closed shell ground state of mercury. Both u_1 and u_2 have a harder repulsion part than the pair potential of open shell heavy alkali metals in accord with the results obtained by the inversion method using experimental pair correlation function.[12]

From the model outlined above, the isotherm thus obtained for the metal state is in the form

$$(Z - 1)V^3 = A\rho^2 + B \tag{3}$$

where Z is the compression factor and V is the molar volume. Constants A and B depend on temperature and are a measure of repulsion and attraction parts of the potential function u_1, respectively. Equation 3 indicates that isotherms of $(Z - 1)V^3$ are linear functions of ρ^2. Notice that for the metal state, a pure metal interaction is assumed, where often a pseudopotential is applied for first principle calculation.[14] The form of $f(\rho)$ restrains the application isotherm (3) to the metal state for $\rho \geq 11$ g/cm^3. From the low-density side of the domain (see eq 2), this isotherm tends to the isotherm with characteristic mixed potential functions u_1 and u_2. Determination of the parameters of the isotherm (3) at a given temperature leads to the calculation of molecular parameters of the corresponding metal potential function:

$$\epsilon_m = \frac{2RT}{5N_A}\left(\frac{B^5}{A^3}\right)^{1/2}, \quad \sigma_m = K_{cell}\left(\frac{-3A}{5B}\right)^{1/6}, \quad (r_{min})_m = ({}^5/_3)^{1/6}\sigma_m \tag{4}$$

where ϵ is the potential well-depth, N_A is Avogadro's number, σ is the hard-sphere diameter, the subscript m stands for the metal state, and RT has its usual meaning. K_{cell} is a constant characteristic of unit cell and can be determined analytically if the unit cell assumed for the metal fluid system is known. In this investigation, its form consists of $K_{cell} = r_{min}/V^{1/3}$, where r_{min} is the interatomic distance at the potential minimum.

For the nonmetal state, the linear isotherm is derived in the form

$$(Z - 1)V^2 = C\rho^2 + D \tag{5}$$

where C and D are constants characteristic of repulsion and attraction of the potential function u_2, respectively. Equation 5 indicates that ρ^2 dependence of $(Z - 1)V^2$ is linear with slope C and intercept D. Again, one would expect to calculate the molecular potential parameters for u_2 with reasonable accuracy by using the constants of isotherm (5):

$$\epsilon_n = \frac{RTD^2}{2N_AC}, \quad \sigma_n = K_{cell}\left(\frac{-C}{2D}\right)^{1/6}, \quad (r_{min})_n = 2^{1/6}\sigma_n \tag{6}$$

where subscript n stands for the nonmetal state. Contrary to the simple form of isotherms for metal and nonmetal states, the isotherm of the metal−nonmetal transition state represents the complexities inherent to the transition state in the form

$$(Z - 1)V^2 = E\rho^4 + F\rho^3 + G\rho^2 + H\rho + I \tag{7}$$

where *E*, *F*, *G*, *H*, and *I*, are constants characteristics of the molecular parameters of LJ(12−6) and LJ(15−9) potential functions.

The consistency of experimental data with the suggested potential function indicates that the effective interaction in the metal state is shorter in range than that of the nonmetal state. This is probably due to the density effect. That is, in the dense metal state the correlation between atoms is high, leading to a highly ordered system, whereas in the nonmetal state the correlation is poor and thus the electrostatic fields of charged species extend readily over several atomic diameters. Experimental data also state that as the temperature is increased the intermolecular distance does not change much but the coordination number decreases.[22] This is consistent with our finding based on the application of u_1 and u_2 which leads to isotherm (7) with

$$E = \frac{15}{2}\left(\frac{200.6}{3\times 10^6}\right)\left(\frac{5}{3}\right)^{3/2}\frac{N_A\epsilon_m}{RT}\left(\frac{\sigma_m}{K_{cell}}\right)^{15} \tag{8}$$

$$F = -\left(\frac{50}{3}\right)\left(\frac{5}{3}\right)^{3/2}\frac{N_A\epsilon_m}{RT}\left(\frac{\sigma_m}{K_{cell}}\right)^{15} - 10\left(\frac{200.6}{3\times 10^6}\right)\frac{N_A\epsilon_n}{RT}\left(\frac{\sigma_n}{K_{cell}}\right)^{12} \tag{9}$$

$$G = -5\left(\frac{5}{3}\right)^{3/2}\left(\frac{200.6}{3\times 10^6}\right)\frac{N_A\epsilon_m}{RT}\left(\frac{\sigma_m}{K_{cell}}\right)^{9} + \left(\frac{88}{3}\right)\frac{N_A\epsilon_n}{RT}\left(\frac{\sigma_n}{K_{cell}}\right)^{12} \tag{10}$$

$$H = 10\left(\frac{5}{3}\right)^{3/2}\frac{N_A\epsilon_m}{RT}\left(\frac{\sigma_m}{K_{cell}}\right)^{9} + 6\left(\frac{200.6}{3\times 10^6}\right)\frac{N_A\epsilon_n}{RT}\left(\frac{\sigma_n}{K_{cell}}\right)^{6} \tag{11}$$

$$I = -\left(\frac{44}{3}\right)\frac{N_A\epsilon_n}{RT}\left(\frac{\sigma_n}{K_{cell}}\right)^{6} \tag{12}$$

4. Results and Discussion

The atomic vapor state of mercury can be described by the same type of interaction potential as simple fluids and a Lennard-Jones (12−6) potential function is applicable. This means the law of corresponding states is applicable to the atomic mercury vapor as well as simple fluids. However, the deviation from this behavior is seen as temperature is increased. The reason for these deviations is that the internal degrees of freedom of mercury atom can be excited, and in particular ionization occurs.[3] For an accurate theoretical treatment, an ionization equilibrium between Hg and Hg^+, Hg^{2+}, and e^- has been assumed, and association processes leading to Hg_2 and molecular ions Hg_2^+ have been included.[3] Therefore, for the details of metal−nonmetal transition in a more rigorous microscopic treatment of mercury fluid, the change of internal degrees of freedom must be considered. Then the interaction potential itself becomes dependent on density and temperature.

Repulsion branches of effective ion−ion potential of mercury and LJ (*m*−*n*) potential with $m > 12$ are almost identical with hard sphere potential, and thus independent of density. This feature actually leads to the application of hard sphere potential for most practical purposes.[3] The interionic potential at freezing temperature is purely repulsion around nearest-neighbor distance. The attraction branch changes from that of a screened Coulomb interaction in liquid to an induced dipole−dipole interaction characteristic of a nonmetal in the atomic vapor state.

In a preliminary consideration for evaluation, we have applied to liquid mercury LJ(12−6) and LJ(6−3) potential functions, which have been shown to be applicable to normal liquids and liquid cesium metal, respectively. The resulted isotherms are shown in Figures 1 and 2 for metal, nonmetal, and transition states. The experimental $P\rho T$ tabulations measured for mercury have been used.[23] [The selected data from available data are in the pressure range 200−5000 atm at $T = 273.15$ K and 3500−5000 atm at $T = 2123.15$ K; the data used for other isotherms given below are selected so as to follow the constraint for $f(\rho)$ in (2).] Both potential functions result in isotherms that are linear from 273.15 up to 1173.15 K. This temperature range corresponds to the (available) density 13.85−11.18 g/cm^3 of the compressed liquid mercury. It is concluded that for fluid densities larger than 11 g/cm^3 both isotherms are perfectly linear. In the same way, the isotherms tend to a linear behavior as the critical point is approached and the liquid−vapor phase transition is occurred. As we see later this corresponds to the liquid with $\rho < 8$ g/cm^3. However, both isotherms markedly deviate from linear behavior in the metal−nonmetal transition region, indicating that a particular force law governs the thermodynamic properties.

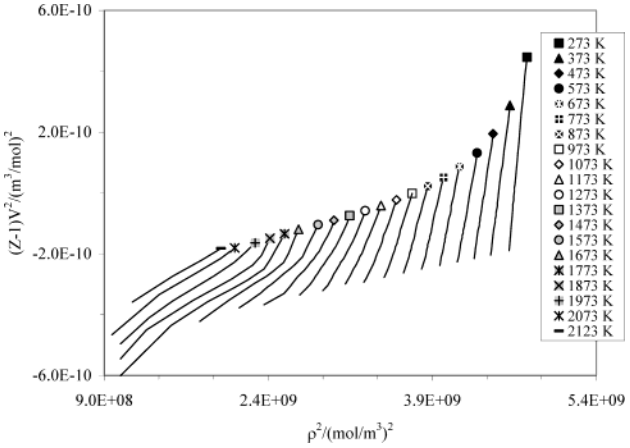

Figure 1. Application of the isotherm of nonpolar, nonmetal fluids to compressed fluid mercury over metal, nonmetal, and metal−nonmetal transition states. The deviation from linear behavior is enhanced most in the transition state.

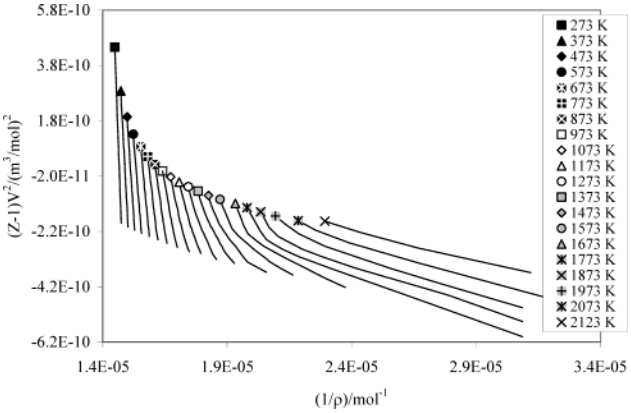

Figure 2. Application of the isotherm of cesium metal fluid to compressed fluid mercury over metal, nonmetal, and metal−nonmetal transition states. The deviation from linear behavior is enhanced most in the transition state. The range of linear behavior in the nonmetal state is more enhanced than in Figure 1.

The properties of liquid mercury such as electrical conductivity indicate metal properties in the former range and nonmetal properties in the later range. Simultaneous measurement of density and electrical conductivity of compressed liquid mercury have been performed by Yao and Endo.[24] They have presented results of their measurements by graphs. The result are limited to transition state (e.g., density range 8−12 g/cm^3 corresponding to the temperature range 1273−1773 K and up to 2200 atm).

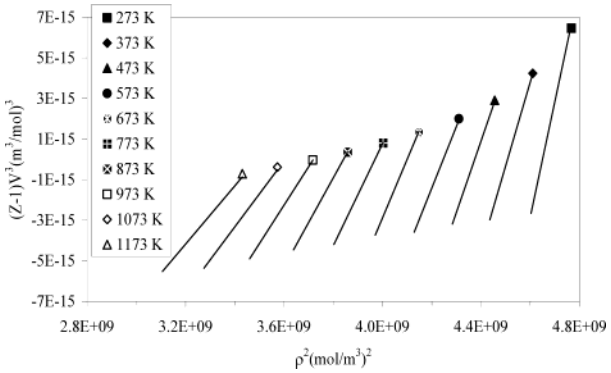

Figure 3. Plots of isotherms of eq 3 in the density range where the metal behavior is enhanced. The plots are subjected to the restriction of $f(\rho)$ in (2).

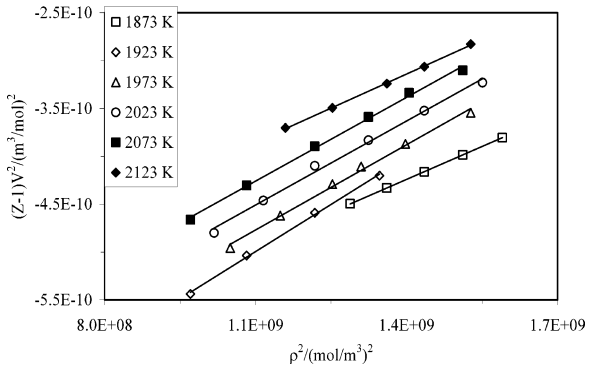

Figure 4. Plots of isotherms of eq 5 for the nonmetal state. The plots are subjected to the restriction of $f(\rho)$ in (2).

Electrical conductivity shows a singularity at 1753 K corresponding to the density in the range 9−8 g/cm^3. Below this temperature, the electrical conductivity represents a certain regime which can be attributed to a metal state, but above this temperature not enough data are given to allow making a clear conclusion about the nature of the (nonmetal) state. The same singularity and behavior are seen from pressure variation of density.[24] Therefore, as long as the fluid system consists of pure identical particles interacting with the same force law, the same power law strictly governs the thermodynamic properties.[25]

The isotherms of eq 3, which have been resulted by using LJ(15−9) as the effective pair potential in metal state, are shown in Figure 3. The reason for selecting such a potential function with hard repulsion is the closed shell 6s^2 electronic structure. In other words, the major interaction in liquid mercury (in the metal state) is due to screened ion−ion, which can be described by a hard repulsion branch. Indeed we have applied LJ (15−9) to produce an accurate equation of state for the metal state, and additionally to yield an analytical equation of state, which could fit suitably the experimental PρT data in the metal−nonmetal transition region. (See next paragraph.)

The isotherms of eq 5 for which supercritical $P\rho T$ data of compressed mercury have been used are shown in Figure 4. Our considerations show that the linear behavior persists well if, at a given temperature, only data with ($5.8 < \rho \leq 8$) g/cm^3 are included, where the lower limit is the critical density ρ_c. This density limit is rather sharp so that the linear behavior deteriorates extensively, otherwise. This indicates that for $\rho \leq 8$ g/cm^3 the fluid mainly consists of neutral atoms with induced dipole−dipole interaction. Our finding is consistent with the literature report in which the nonmetal state is described well by the LJ(12−6) potential function.[3,12]

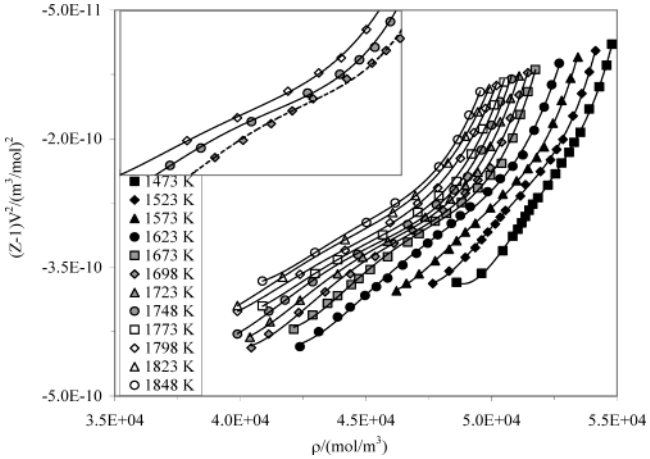

Figure 5. Plots of isotherms of eq 7 for the metal−nonmetal transition range. The inset shows enhancements of isotherms at 1698, 1748, and 1798 K.

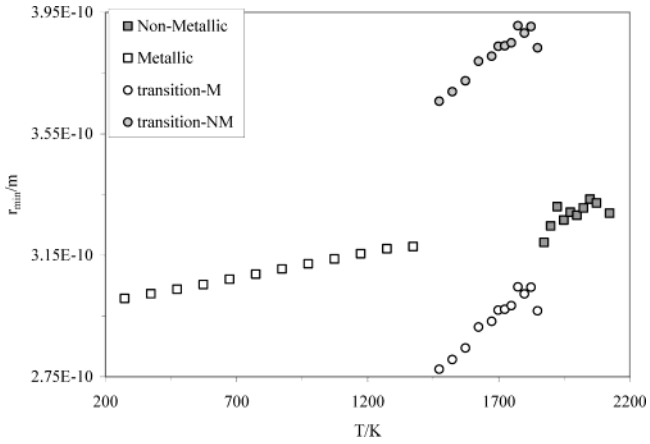

Figure 6. Plots of r_{min} vs T for metal, nonmetal, and transition states. The two plots in the transition region result from solution of the relations 8−12.

The success of the present work can be attributed to the derivation of the fourth-order eq 7 as the equation of state for the metal−nonmetal transition range (see Figure 5). From the available experimental data, we have chosen the temperature range (1473.15−1848.15 K) which includes the low-density metal state and the high-density nonmetal state to test this equation of state. In the insert of Figure 5, the density variation of $(Z - 1)V^2$ shows an enhancement of inflection point from a metal branch to a nonmetal one. In particular, at 1748.15 K there is a marked inflection point, though all isotherms show such a behavior slightly.

The value of r_{min} calculated for metal, nonmetal, and metal−nonmetal transition regions are shown in Figure 6. We have used values of r_{min} from the plots of pair correlation function vs interatomic distance,[2] determined at saturation pressures, and have calculated K_{cell}. We have noticed that K_{cell} remains almost constant over the whole liquid range. This may be attributed to the fact that K_{cell} is proportionality constant between two characteristics parameters of the fluid system, and thus we have applied this value, despite the fact we are confronting the problem of applying a saturation property to solve for properties at compression, in all calculations. The typical calculated value of r_{min} at 273.15 K is 3.00 Å, which is in excellent agreement with experimental value of 3.01 Å (within 0.33%).[26] Thus, the method of this study reproduces the molecular potential parameter r_{min} reasonably accurate. The experimental value of r_{min} (and ϵ/k as well) have been determined by integration using

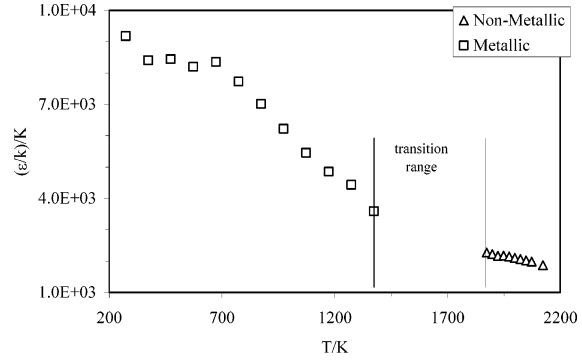

Figure 7. Plots of (ϵ/k) vs T for metal and nonmetal states. No coordination numbers were applied.

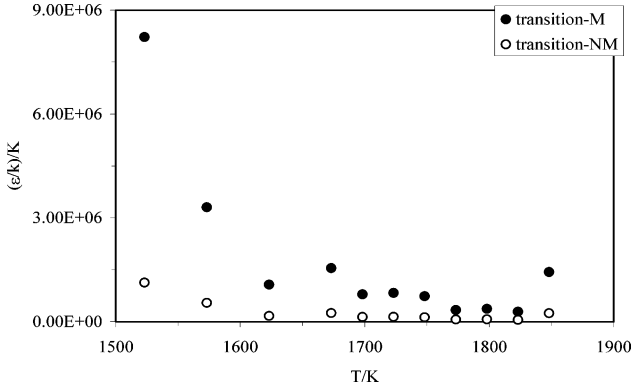

Figure 8. Plots of (ϵ/k) vs T for the metal−nonmetal transition range. The two plots are for the transition region, and they resulted from simultaneous solution of the relations 8−12.

available experimental second virial coefficient of mercury and LJ (12−6) potential function.[26] It is noticeable that r_{min} (in this study) increases slightly with temperature (by 5.66%) at T = 1373.15 K (at which the transition is admitted).

The plots of (ϵ/k) vs temperature (with k being the Boltzmann constant) for metal and nonmetal ranges are shown in Figure 7. These values of (ϵ/k) are calculated disregarding the coordination number of liquid mercury. For the metal state, we have calculated (ϵ_m/k) by using eq 4 along with isotherm (3). The coordination number of mercury has been determined experimentally at saturation pressures,[27] and typically equals 9.36 at 13.55 g/cm^3 corresponding to T = 273.15 K . Thus, for a pair of mercury atoms at this temperature, $(\epsilon_m/k)_{calcd}/(\epsilon/k)_{expt}$ = 981/1030 = 0.952, where $(\epsilon/k)_{expt}$ is the reported molecular potential parameter of LJ(12−6) obtained by using the second virial coefficient.[26] Notice that at T = 273.15 K the available $P\rho T$ data are in the range 200−5000 atm. On the other hand, at T = 1873.15 K, $P\rho T$ data are available in the pressure range 2200−5000 atm; however, the data in the range 2200−2600 atm have been applied to follow restrictions for f(ρ) in (2). This excludes also densities less than the critical density ρ_c = 5.8 g/cm^3. At this temperature $(\epsilon_n/k)_{calcd}/(\epsilon/k)_{expt}$ = 428.3 K/1030 K = 0.416, for which the coordination number equals 5.31.[23] It can be concluded that the method of this study can reproduce reasonably well the molecular parameters of pair potential function at low temperature, which for their calculations subcritical experimental data of compressed liquid mercury, comparable roughly with data at saturation pressures, are involved. [The critical point data are T_c = 1751 K, P_c = 1695 atm, and ρ_c = 5.8 g/cm^3.] At the low temperature, the deviation of the above ratio from unity (e.g., 0.952) can be attributed to the fact that liquid mercury has been investigated at pressures range just somewhat higher than saturation pressures. On the other hand, at high temperature, the large deviation of $(\epsilon_n/k)_{calcd}$ from that of an isolated pair can be attributed to the high pressures (supercritical) data, which pushes a pair of mercury atoms further inside the r_{min} distance with more effective repulsion potential, thus lowering the potential well depth.

Since the analytical form of K_{cell} is not known, we have calculated its value by using reported the experimental r_{min},[2] in $r_{min} = K_{cell}V^{1/3}$ at T = 273.15 K. We have noticed that K_{cell} remains almost constant over the range T = 273.15−2000 K and does not affect the values of $(\epsilon/k)_{calcd}$.

Figure 8 shows the plots of (ϵ/k) vs temperature for the metal−nonmetal transition region obtained by using relations 8−12. Essentially simultaneous solution of eqs 8−12 is appreciated for covering any uncertainty in the values of coefficient in eq 7, which may rise due to unsatisfactory fitting. However, we cannot explain the large differences between $(\epsilon/k)_{calcd}$ and $(\epsilon/k)_{expt}$ by 2 to 3 orders of magnitudes with respect to that of the metal region and 1−2 orders of magnitudes with respect to that of the nonmetal region (see Figure 7). Because ϵ and σ are dependent parameters in the transition region, the metal (nonmetal) value of r_{min} ($\propto\sigma$) in this region is rather smaller (larger) than the corresponding value in the metal (non-metal) region (see Figure 6). A clear explanation for the behavior of either parameter may lead to an understanding of the other one.

From the metal side of the transition region, there exists a step-side rising edge which diminishes sharply as density decreases toward the nonmetal side of the transition region. Despite a lack of a reasonable explanation, this is a singularity characteristic of a phase transition. Interestingly, the experimental bulk viscosity of mercury increases when density decreases to the density of the nonmetal region, and passes through a maximum, almost at the middle of transition region corresponding to 9.5−9.75 g/cm^3.[15] The simulation for bulk viscosity using pseudopotential method and the restriction for $f(\rho)$ result in the same singularity though the rising edge is toward the low-density side of the transition region.

5. Conclusion

Interatomic interaction potential energy functions have been used to derive equations of state in metal, nonmetal, and metal−nonmetal transition states of compressed fluid mercury. Density-dependent potential functions have been used, specifically for the metal−nonmetal transition range of fluid mercury, which has been shown to be limited to density range ($8 < \rho < 11$) g/cm^3. The equations of state for metal and nonmetal states have simple forms, and the complexities associated with the metal−nonmetal transition have led to a rather complex fourth-order equation of state. The values of potential well−depth ϵ in the metal region are in agreement with experimental values typically within 5.0% of an isolated pair of mercury−atom. However, calculated ϵ values of the nonmetal were found to be much smaller than those for a pair of isolated atom, attributing exceedingly large repulsion due to the high pressure $P\rho T$ data used, which pushes atoms further together inside the r_{min} distance. The calculated values of ϵ for transition region show singular behavior characteristics of a phase transition, though we cannot explain a higher 2−3 orders of magnitude value with respect to the metal state. The value of r_{min} for metal state is in agreement with that of an isolated pair within 0.33%. Also in the transition region r_{min} calculated for a nonmetal is higher (but finite value), and at the rising edge, it increases by about 15% with respect to the metal state. Singularities in the transition range in this study have shown enhancement on the energy scale rather than on the structure scale.

Acknowledgment. The authors are indebted to the research council of Shiraz University for supporting this study. They are also grateful to H. Okumura of Keio University for providing a preprint[15] of their studies prior to publication.

References and Notes

(1) Röpke, G.; Nagel, S.; Redmer, R. *Contrib. Plasma Phys.* **1993**, *33*, 441.
(2) Hensel, F. *Adv. Phys.* **1995**, *44*, 3.
(3) Nagel, S.; Redmer, R.; Röpke, G. *J. Non-Cryst. Solids* **1996**, *205*−*209*, 247.
(4) Mansoori, G. A.; Jedrzejek, C.; Shah, N. H.; Blander, M. *Chemical Metallurgy-A Tribute to Carl Wagner*; Gokcen, N. A., Ed., The Metallurgical Society of AIME: New York, 1981; pp 233−240.
(5) Hefner, W.; Shmutzler, R. W.; Hensel, F. *J. Phys. (Paris) Colloq.* **1980**, *41* C8, 62.
(6) Yao, M. *Z. Phys. Chem.* **1980**, *184*, 173.
(7) Yao, M.; Hayami, W.; Endo, H. *J. Non-Cryst. Solids* **1990**, *117*−*118*, 473.
(8) Schonherr, G.; Schmutzler, R. W.; Hensel, F. *Philos. Mag. B* **1979**, *40*, 613.
(9) Even, U.; Jortner, *J. Philos. Mag.* **1972**, *25*, 715; *Phys. Rev. B* **1973**, 2536.
(10) El-Hanany, U.; Warren, W. W., Jr. *Phys. Rev. Lett.* **1975**, *34*, 1276.
(11) Suzuki, K.; Inutake, M.; Fujiwaka, S.; Yao, M.; Endo, H. *J. Phys. (Paris)* **1980**, *41*, C8−66.
(12) Munejiri, S.; Shimoji, F.; Hoshino, K. *J. Phys.: Condens. Matter* **1998**, *10*, 4963.
(13) Hensel, F. *J. Phys.: Condens. Matter* **1990**, *2*, SA33.
(14) Tamura, K.; Hosokawa, S. *J. Phys.: Condens. Matter* **1994**, *6*, 419.
(15) Okurmura, H.; Yanezawa, F. *J. Non-Crystalline Solids* **2002**, *312*−*314*, 260.
(16) Tamura, K.; Inui, M.; Nakaso, I.; Oh'ishi, Y.; Funakoshi, K.; Utsumi, W. *J. Phys.: Condens. Matter* **1999**, *10*, 11405.
(17) Kohno, H.; Yao, M. *J. Phys.: Condens. Matter* **1999**, *11*, 5399.
(18) Gray, P.; Rice, S. *J. Chem. Phys.* **1964**, *41*, 3689.
(19) Ghatee, M. H.; Shams-Abadi, H. *J. Phys. Chem. B* **2001**, *105*, 702.
(20) Ghatee, M. H.; Bahdori, M. *J. Phys. Chem. B* **2001**, *105*, 11256.
(21) Ghatee, M. H.; Bhadori, M. *Fluid Phase Equilib.* **2003**, *205*, 339.
(22) Tamura, K.; Hosokawa, S. *J. Non-Crystalline-Solids* **1993**, *156*−*158*, 646.
(23) Kikoin, I. K.; Senchenkov, A. P. *Fiz. Metal. Metalloved.* **1967**, *24*, 843.
(24) Yao, M.; Endo, H. *J. Phys. Soc. Jpn.* **1982**, *51*, 966.
(25) Keshavarzi, A.; Parsafar, G. *J. Phys. Chem. B* **1999**, *104*, 6584.
(26) Röpke, G.; Negal, S.; Redmer, R. *Z. Phys. Chem. Bd.* **1995**, 192, S.
(27) Tamura, T.; Hosokawa, S. *J. Phys.: Condens Matter* **1994**, *6*, A 241.